

GeoTop: Advancing Image Classification with Geometric-Topological Analysis

Mariam Abaach¹, Ian Morilla^{2,3*}

¹MAP5 UMR CNRS 8145, Université de Paris, 45 rue des Saints-Pères, 75006 Paris, France

²Université Sorbonne Paris Nord, LAGA, CNRS, UMR 7539, Laboratoire d'excellence Inflammex, F-93430, Villetaneuse, France

³University of Malaga, Departments of Genetics, and Applied Mathematics, MLiMO, 29010, Málaga, Spain

November 29, 2023

Abstract

In this study, we explore the application of Topological Data Analysis (TDA) and Lipschitz-Killing Curvatures (LKC) as powerful tools for feature extraction and classification in the context of biomedical multiomics problems. TDA allows us to capture topological features and patterns within complex datasets, while LKCs provide essential geometric insights. We investigate the potential of combining both methods to improve classification accuracy.

Using a dataset of biomedical images, we demonstrate that TDA and LKCs can effectively extract topological and geometrical features, respectively. The combination of these features results in enhanced classification performance compared to using each method individually. This approach offers promising results and has the potential to advance our understanding of complex biological processes in various biomedical applications.

Our findings highlight the value of integrating topological and geometrical information in biomedical data analysis. As we continue to delve into the intricacies of multiomics problems, the fusion of these insights holds great promise for unraveling the underlying biological complexities.

Keywords

Topological Data Analysis, Lipschitz-Killing Curvatures, feature extraction, classification, biomedical multiomics, data analysis.

1 Introduction

Recent advancements in medical imaging have ushered in a new era, empowering healthcare professionals with cutting-edge image processing tools and innovative methodologies. These tools have not only provided invaluable diagnostic assistance but have also facilitated a deeper understanding of disease severity and progression monitoring [1–3]. In this scenario, the integration of multiomics data from various sources has become pivotal for gaining a comprehensive understanding of complex biological systems. Biomedical multiomics problems often involve analysing high-dimensional data, such as genomic, transcriptomic, proteomic, and imaging data, to uncover meaningful patterns and associations. To address the challenges posed by this data deluge, advanced data analysis techniques are required.

Topological Data Analysis (TDA) and Lipschitz-Killing Curvatures (LKC) have emerged as powerful tools for the analysis of complex and high-dimensional datasets. TDA focuses on capturing topological features and structures within data, providing a means to unveil hidden patterns and relationships. LKCs,

*Corresponding author: morilla@math.univ-paris13.fr

on the other hand, offer a unique perspective by emphasising the geometric aspects of data, enabling the extraction of essential structural information.

This research explores the potential of TDA and LKCs in the realm of biomedical multiomics. We investigate their capabilities for feature extraction and classification, with a particular emphasis on image analysis. Images play a crucial role in biomedical research, providing valuable insights into cellular and tissue structures. Extracting meaningful features from these images and accurately classifying them is essential for tasks such as disease diagnosis and drug discovery.

Our primary mission revolves around a classification task, where we systematically evaluate the performance of two distinct sets of feature—geometrical and topological. By rigorously assessing the strengths and weaknesses of each feature set, we delve into the intriguing realm of supervised classification. Yet, our quest does not stop here; we also embark on an exploration of the synergistic potential inherent in the fusion of geometry and topology. Through this comprehensive analysis, we seek to unearth the untapped benefits that combining these two domains can offer within the context of supervised classification.

In this paper, we present a detailed analysis of our experimental results, demonstrating the effectiveness of TDA and LKCs in extracting relevant features from biomedical images. We also highlight the improvements achieved by combining these methods. Our findings have the potential to contribute significantly to the field of biomedical data analysis, offering new avenues for gaining insights into complex biological systems.

The remainder of this paper is organised as follows: In Section 2, we provide an overview of the theoretical foundations of TDA and LKCs. Section 3 describes the dataset and methodology used in our experiments. Section 4 presents the results and discusses the implications of our findings. Finally, in Section 5, we offer a conclusion and outline future research directions.

This research journey holds the promise of not only advancing the field of medical image analysis but also shedding light on the transformative potential of interdisciplinary approaches, where geometry and topology converge to enhance our understanding and classification of complex medical data.

2 Mathematical Preliminaries

In this section, we revisit fundamental concepts and definitions that serve as the foundation for understanding persistent homology and persistent diagrams (PDs).

2.1 Introduction to Topological Data Analysis

Topological Data Analysis (TDA) is a burgeoning field that equips us with mathematically rigorous techniques to uncover the intricate topological structures hidden within datasets. These structures are then distilled into quantitative and qualitative features that can be harnessed for a myriad of machine learning tasks. TDA’s versatility shines through as it can adeptly mine underlying topological patterns across diverse applications, spanning classification, segmentation, and clustering. In our research, our paramount focus is on the application of TDA to the realm of image processing, where we aim to harness topological features for tasks such as classification and segmentation. Notably, while images inherently exhibit a grid-like structure, the utilisation of TDA in image processing represents a relatively recent frontier in computational analysis [4].

The pioneering applications of TDA in image processing trace back to seminal work [5], where topological methods were deployed to distinguish core regions from smaller ones within images for classification purposes. In the medical domain, TDA has left a profound impact as exemplified by studies such as [6] and [7], which leveraged TDA to enhance the identification and segmentation of critical objects in medical images. These efforts culminated in an unsupervised method for skin lesion image segmentation. Furthermore, recent advancements include [8], where TDA was applied to tumor CT scans, showcasing its potential to predict survival rates in lung cancer patients. Building upon this, [9] extended TDA’s utility to thoracic radiographic images for lung tumor histology prediction, revealing improved classification between malignant and benign tumours when combined with radiomic features. A striking example can be found in [10], where TDA was employed to segment skin cancer images and classify various types of skin lesions. As a result, TDA has become a staple in the machine learning toolkit for summarising both global and local topological data features, often without the need to delve into the underlying geometric characteristics.

Our research embarks on this journey by introducing a fundamental concept from Topological Data Analysis known as “persistent homology”. This method excels at extracting topological features that are pivotal for our classification tasks. Persistent homology empowers us to infer the so-called “homology groups” of a dataset. In our exposition, we prioritise clarity and accessibility, opting for illustrative examples over formal definitions, ensuring that even those without prior knowledge of homology groups can grasp the essentials [11]. For those seeking a deeper understanding of persistent homology, we provide references to authoritative sources like [12]. Following this introduction, we delve into the geometrical model, seamlessly integrating geometric features within our bivariate framework [13]. These features encompass area, perimeter, and Euler characteristic, each contributing unique insights. Subsequently, we feed these features into a supervised machine learning classifier to discern two-dimensional skin cancer data. Our rigorous approach involves a meticulous comparison of the individual performance of each model and a comprehensive assessment of the enhancements achieved when both geometric and topological features are synergistically employed.

It is vital to underscore that TDA often complements other machine learning models, enhancing their performance and offering additional insights. In our study focusing on skin cancer data, our goal is to explore the potential advantages of combining geometric and topological models for classification tasks. Importantly, our aim is not to replace other machine learning techniques but rather to complement them. We aspire to unveil concealed topological and geometric facets that can enrich the classification process. Therefore, by amalgamating TDA with geometric features such as area, perimeter, and Euler characteristic, we seek to evaluate each model’s performance in isolation and ascertain the benefits derived from leveraging both geometry and topology.

3 Methodology and Algorithm

The following section provides a step-by-step account of our research methodology, from data acquisition and preprocessing to feature extraction, classification, and the exploration of combined TDA and LKCs. This comprehensive methodology serves as the foundation for our research, facilitating a clear understanding of the techniques employed and their potential impact on biomedical multiomics problems.

3.1 From an Image to a Persistence Diagram

In our research, we focus on the application of TDA in the field of image processing. This section provides a concise overview of the TDA process when applied to images. For a more comprehensive and detailed presentation of this process, we recommend referring to [14].

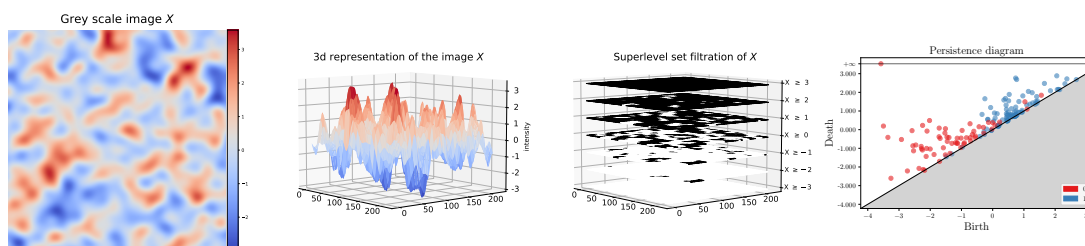


Figure 1: Extraction of the topological feature from a grayscale image X.

The entire process of extracting topological features from these binary images is known as persistent homology, a fundamental and widely utilised technique in TDA. Persistent homology provides a robust theoretical framework that enables us to infer the *homology group* of a given dataset. Traditionally, persistent homology has been applied primarily to point cloud data, but its applicability extends to images, capitalising on their inherent cubical structure.

(Static) Homology Groups

Homology serves as a foundational concept in algebraic topology, offering a powerful means to formalise and represent the topological characteristics of a given space in an algebraic framework. It operates as a

mathematical tool that translates topological spaces into vector spaces, particularly in our context, $\mathbb{Z}/2\mathbb{Z}$ -vector spaces. This transformation results in a sequence of vector spaces, each of which encodes specific topological features. For any dimension k , homology allows us to detect and quantify the presence of k -dimensional “holes” in the space. These holes are precisely characterised by vector spaces denoted as H_k and are referred to as *homology groups*. The dimension of H_k intuitively corresponds to the count of independent features or “holes” of k -dimensionality within the space. To illustrate, the 0-dimensional homology group H_0 represents the connected components of the space, while H_1 captures 1-dimensional loops, and H_2 characterises 2-dimensional cavities, and so forth. For a comprehensive understanding of the rigorous construction of these groups, we direct the interested reader to [12], which offers a thorough presentation of homology theory and algebraic topology.

In order to compute the homology of a space, it must possess a defined topological structure. Unfortunately, grayscale images lack an inherent topological structure. As a workaround, we can consider a fixed threshold $t \in \mathbb{R}$ and generate the associated black-and-white image. The set of white pixels in this image, referred to as the excursion set, denoted as $\mathcal{X}_t(X) = \{x \in \mathbb{G}_m, X_x \geq t\}$, forms a subset of \mathbb{G}_m . This subset inherits its topological structure, enabling us to compute the homology groups (H_k) of $\mathcal{X}_t(X)$.

Furthermore, within the realm of homology, the concept of *cubical homology*, as described in [15], offers a well-suited approach for image analysis. This method transforms binary images, which can be envisioned as unions of cubes, into vector spaces. To illustrate this, consider Figure 2, where the black and white image exhibits three independent features in dimension 0, each corresponding to a connected component, and two holes in dimension 1, representing the cycles enclosed within the empty circles.

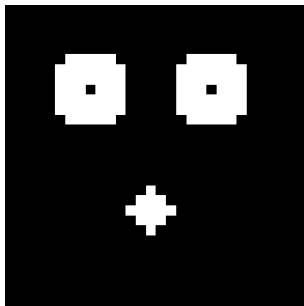


Figure 2: Black and white image of size $m = 30$, $\dim(H_0) = 3$, $\dim(H_1) = 2$

Persistent Homology and Persistence Diagram

Instead of considering only a single threshold, a more versatile approach involves iterating through all the pixel values of the image X , thereby generating a series of black and white images $(\mathcal{X}_t(X))_{t \in \mathbb{R}}$. This iterative process allows us to observe the evolution of the homology groups throughout this entire range. The knowledge of this sequence of sets $(\mathcal{X}_t(X))_{t \in \mathbb{R}}$ not only enables the reconstruction of the original image X but also encapsulates a wealth of topological and geometrical information.

The variant of homology under consideration, denoted as persistent homology, diverges from classical homology by its ability to delineate the dynamic evolution inherent in a complex system. Specifically, in order to monitor the progression of homology groups, it becomes imperative to establish an ascending series of binary images. Within this context, an “increasing family” conveys that once a pixel becomes active (transforms to white) at a given threshold t , it must sustain its activity for all subsequent thresholds $s \leq t$. In essence, the emergence of a topological feature necessitates a perpetual presence; it either endures without alteration or perpetually expands until confluence with another feature. To ensure this systematic advancement, a traversal through image values occurs from maximum to minimum, effectively encompassing the entire spectrum of threshold values from $+\infty$ to $-\infty$. For any two values s and t in \mathbb{R} , where $s \leq t$, it follows that $\mathcal{X}_t(X) \subseteq \mathcal{X}_s(X)$, yielding an expanding family of binary images parameterized by t . This ensemble is denoted as the “superlevel sets filtration” of X . Analogously, by considering the set of pixels with intensities lower than or equal to t , the “sublevel sets filtration” of X is derived, as depicted in Figure 3.

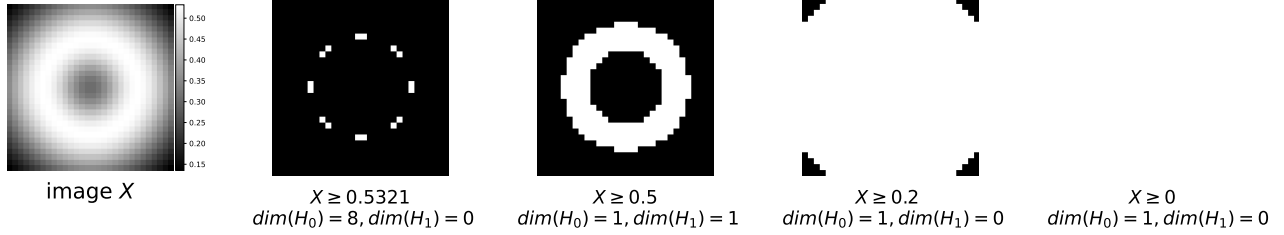


Figure 3: Superlevel filtration of the image X .

In accordance with Figure 3, the parameter t assumes a temporal character, with pixels of higher values activating initially. This implies that the brightest regions of the image manifest first in the filtration sequence, while the darker regions gradually emerge. Eventually, every pixel in the image becomes part of this process. This approach facilitates the tracking of topological features within the filtrations. A feature may make its initial appearance (birth) at time t_b and evolve until it merges with another feature (death) at time t_d . The cessation of a component only transpires upon merging with another. In such instances, the surviving component is designated as the elder of the two. This dynamic unfolding of connected components' lifespans is documented in what is termed a “persistence barcode.” Subsequently, the birth and death coordinates of these features find representation in a visual format known as a “persistence diagram.”

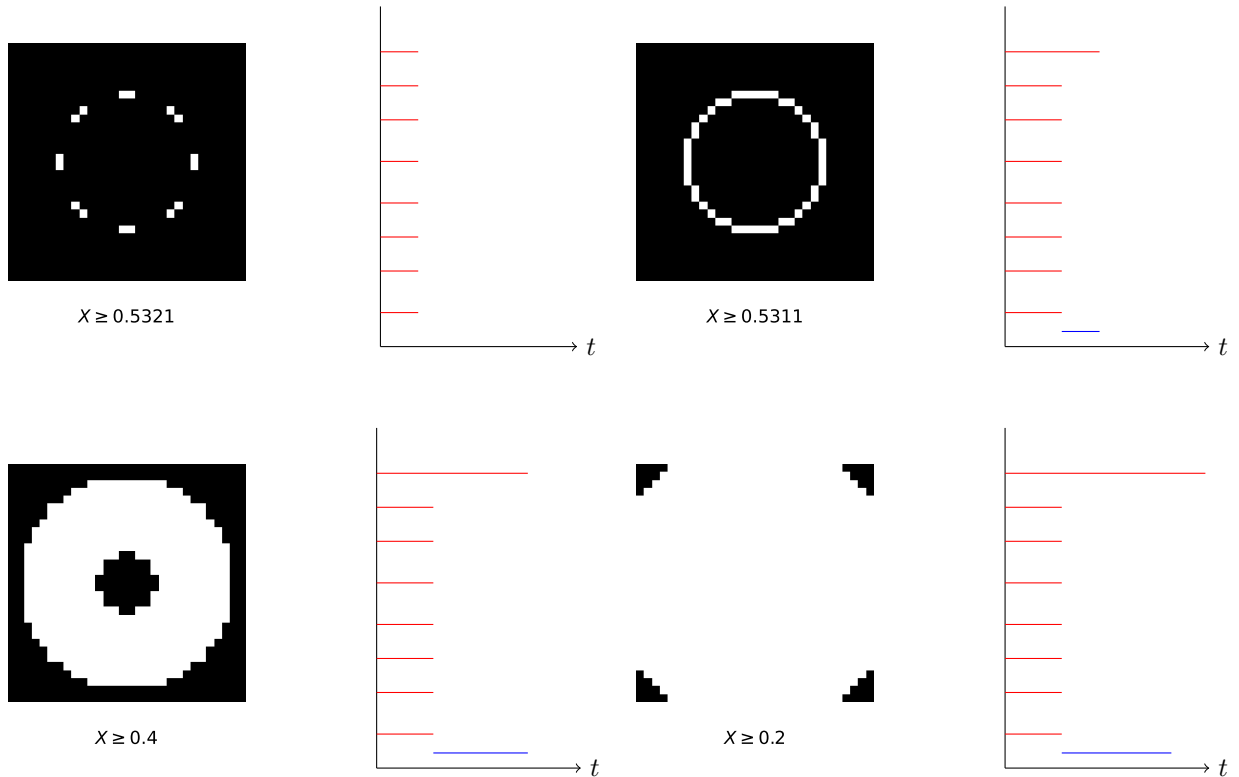


Figure 4: Capturing the changes of the topological features in $\mathcal{X}_t(X)$ as the threshold t evolves.

In Figure 4, each horizontal bar serves as a representation of a topological feature. The color assigned to each bar corresponds to the dimension of the feature, with red indicating an H_0 component and blue representing an H_1 component. The initiation of a bar marks the birth of the respective feature, while its termination signifies the moment of its demise. Features cease to exist either when two components merge together or when a cycle in H_1 becomes fully enclosed. The length of each bar provides a visual representation of the feature’s lifespan, reflecting the duration from its inception to its conclusion. This

interval, during which a feature persists, is referred to as its *persistence*.

In practical terms, features with significant persistence are interpreted as meaningful and relevant characteristics within the data set, often denoting significant patterns or structures. Conversely, features with low persistence are typically regarded as noise or insignificant fluctuations and are often filtered out. Ultimately, as the filtration process continues, all features will eventually cease to exist, except for one. This sole surviving component represents the final and most persistent topological structure.

These features are then condensed into a persistence diagram, as depicted in Figure 5. In the diagram, each feature is summarised as a point. The distance of a point from the diagonal line reflects the feature’s persistence in the image. Points that are closer to the diagonal line are indicative of short-lived or low-persistence features and are often considered as noise. In contrast, points farther from the diagonal represent highly persistent and significant topological structures. As illustrated in Figure 5, the image contains only two crucial topological features: one connected component and one hole. This observation is derived from the fact that the seven other connected components merge and vanish rapidly during the filtration process.

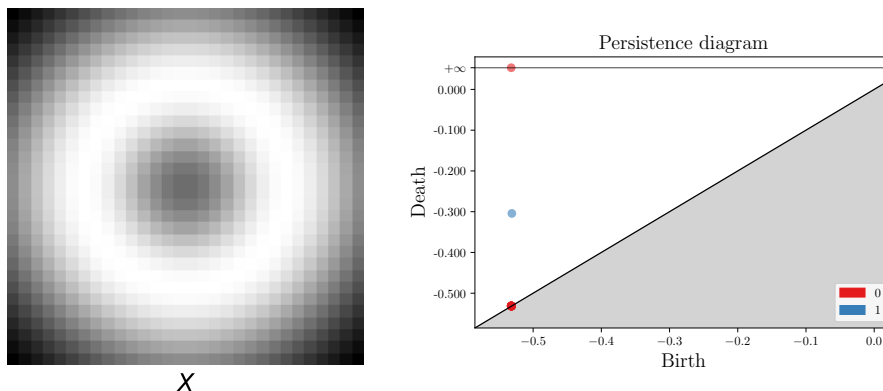


Figure 5: The persistence diagram of the image X .

3.2 Lipschitz-Killing Curvatures

Lipschitz-Killing Curvatures (LKC) represent a sophisticated and widely employed class of geometric summarisation tools. Traditionally, the focus has been on the theoretical examination of individual LK Curvatures. However, recent theoretical developments, as seen in [16] and [17], have aimed to explore the collective behaviour of LK Curvatures within excursion sets.

The significance of investigating the geometry of random sets can be traced back to Hadwiger’s characterization theorem, which positions LKCs as fundamental components of all rigid motion invariant valuations of convex bodies. Consequently, LKCs offer concise and insightful insights into the spatial characteristics of the random fields under scrutiny.

In this study, our research concentrates on the two-dimensional domain, specifically random fields defined on \mathbb{Z}^2 . Within this context, to describe the geometry of excursion sets of random fields, we have access to three distinct LKCs: the area of the set, the perimeter, and the Euler-Poincaré characteristic. The latter is equal to the number of connected components minus the number of holes within the excursion set and serves as a topological invariant. Each of these geometrical features captures different aspects of spatial properties:

- The surface area is linked to the occupation density.
- The perimeter reflects the regularity of the set.
- The Euler characteristic denotes the level of connectivity.

LKCs, therefore, emerge as powerful tools for providing meaningful and concise summaries of the spatial properties exhibited by the random fields under investigation.

This study seeks to explore the insights offered by both methods individually and their potential synergy. Comparing these approaches can reveal their unique contributions and benefits, fostering a more comprehensive understanding of their combined capabilities.

3.3 Presentation of the Dataset

The dataset comprises a balanced collection of benign and malignant skin moles, with images of dimensions (3, 224, 224). It includes 1800 benign moles and 1497 malignant ones, and it was made available by *The International Skin Imaging Collaboration* and can be found on the *Kaggle* website under the name *Skin Cancer: Malignant vs. Benign*.

We initiate the dataset preprocessing by ensuring that the tumor occupies the highest pixel values in the image, with the lowest values designated for the background. Subsequently, we center and normalise the images.

Figure 6 presents grayscale representations of two images from the dataset: one depicting a benign mole and the other a malignant tumor, along with their respective excursion sets. In this representation, black signifies pixels with a value of 0, while white represents pixels with a value of 1. During the iterative thresholding process, as we progress from the highest to the lowest image values to construct the filtration, only pixels belonging to the mole become activated, distinguishing them from the background. By the end of the process, all pixels become white as we reach the minimum image value.

3.4 Extraction of Topological and Geometrical Features

Feature extraction was performed on all three RGB channels in addition to the grayscale image.

Topological Features Following the approach outlined in [4], we extract the topological characteristics of the images to construct a feature vector for input into the machine learning model. To accomplish this, we utilise the Python module `gtda.images`, which offers a suite of tools for applying TDA to images.

We adopt the natural filtration of the image (as described earlier) and begin by employing the `gtda.homology.CubicalPersistence` function. This step enables us to construct persistence diagrams for dimensions 0 and 1, following the pipeline outlined in [4]. In this pipeline, the *amplitude* of a persistence diagram is defined as its distance from the empty diagram, which contains only the diagonal points.

To compute feature vectors, we consider all available metrics within the Python module to calculate the norm of the diagrams. Each persistence diagram is associated with 7 amplitudes and the entropy of the diagram, resulting in a total of 8 features per image channel (grayscale, red, green, blue) per dimension of the diagram. This results in a total of 64 features per image for classification purposes.

In Figure 7, we provide visual examples of a persistence diagram and barcode for grayscale images of both benign and malignant tumours.

In [4], due to the low range of values in the database under study, they initially binarise the images before reconstructing the grayscale-associated images to apply the TDA pipeline.

Geometrical features After a series of trial and error experiments, we have established a set of thresholds denoted as T , comprising 200 equidistant points ranging from the minimum to the maximum values of the images and their corresponding excursion sets. From these, we compute three scaled geometrical features: area (\mathcal{A}), perimeter (\mathcal{P}), and Euler characteristic (\mathcal{E}), with $LKC = \frac{LKC}{m^2}$.

The area is determined by summing the white pixels in an image, while the perimeter is calculated using the algorithm introduced in the Introduction, based on the work [18]. The Euler characteristic is computed using the method presented in [19].

For each geometrical function and its respective derivative, we apply a series of methods from the Python libraries Numpy and Scipy to summarize them. Through experimentation, we have identified the methods that yield the best classification results. Let f denote one of the LKC functionals, and ∂f its derivative. We employ the following techniques:

- L2 norm of \check{f} and ∂f computed using `numpy.linalg.norm(., ord = 2)`.
- Integral of \check{f} and ∂f computed using `numpy.trapz(., T)`.

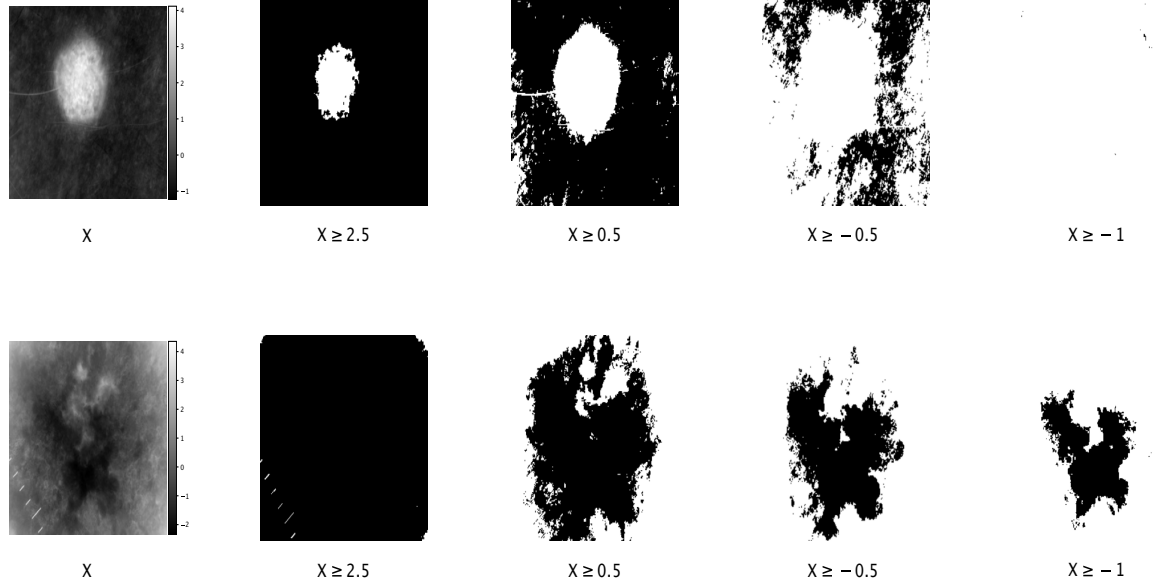


Figure 6: Grayscale image of a benign (top row) and malignant tumour (bottom row) along with their respective excursion sets.

- Sum of all values of \check{f} , $\sum_{t \leq 200} \check{f}(t)$.
- Entropy value of $|\check{f}|$ and $|\partial \check{f}|$ computed using the `scipy.stats.entropy` function.
- Number of non-zero values in \check{f} and $\partial \check{f}$ using `numpy.linalg.norm(., ord = 0)`.
- Sum of \check{f} and $\partial \check{f}$.

Although the sum and the integral may seem to provide similar numerical information, we observed that using both improves the classification performance by 0.2% and reduces the number of false negatives in this method.

In total, we obtain 120 features per image, which are then used as input for the random forest classifier.

Figure 8 reveals that the data is positively shifted and not centred, indicating a departure from Gaussian behaviour.

Additionally, we explore a method where we concatenate both the topological and geometrical feature vectors to investigate whether combining both approaches can enhance classification accuracy. We refer to this third method as GeoTop.

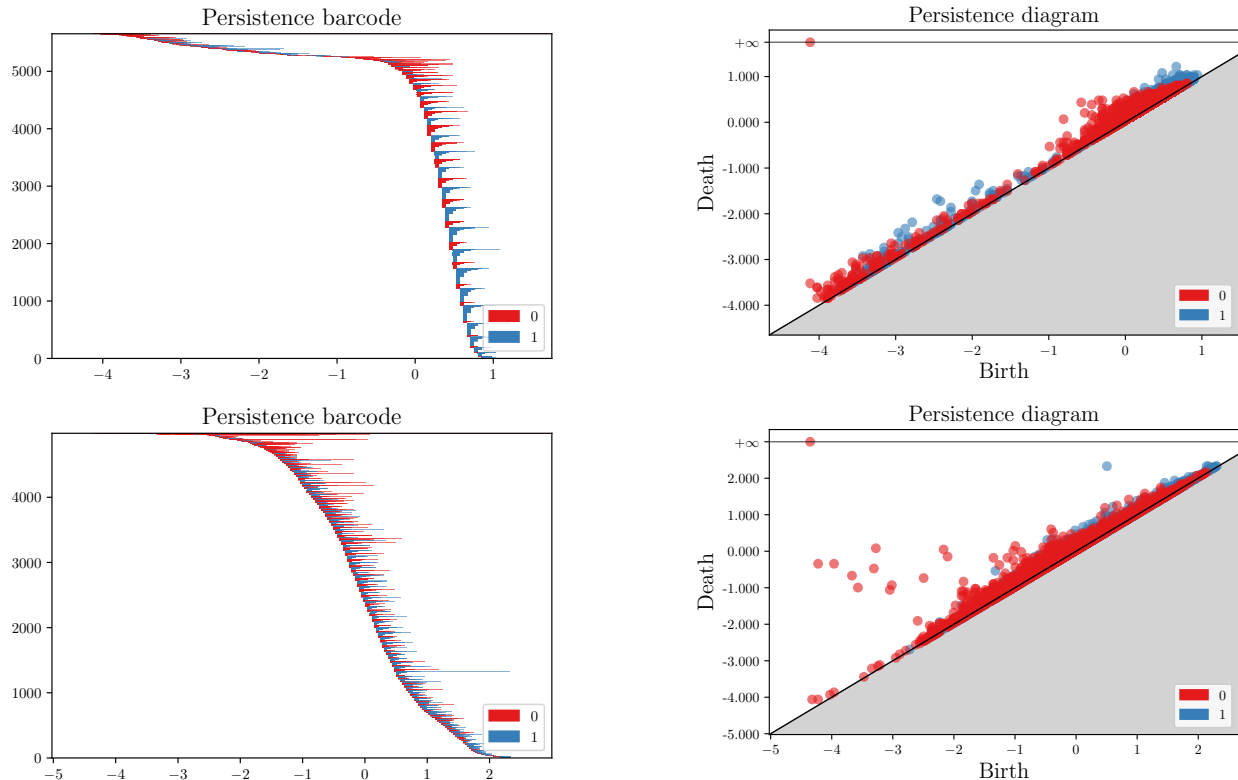


Figure 7: Examples of persistence diagrams and barcodes for grayscale images of benign (top row) and malignant (bottom row) tumours.

4 Results

This section offers a detailed examination of our experimental findings, shedding light on the synergy between TDA and LKCs in biomedical image analysis. These insights pave the way for the development of our methodology that can contribute to a deeper understanding of intricate biological processes and enhance the capabilities of biomedical research and diagnostics.

4.1 Machine Learning Model

We chose to employ a simple random forest classifier to evaluate and compare the performance of the two methods. Our approach involves bootstrapping, where we divide the dataset into 80% training data and 20% testing data. We train and test each of the three models (TDA, LKC, and *GeoTop*) on the same training and testing datasets for patients. We repeated this process 500 times, thereby collecting 500 scores computed using the ‘score’ method of the ‘RandomForestClassifier’ class from the ‘sklearn.ensemble’ module. In Table 1, we present the mean values of the scores and their corresponding standard deviations, while Figure 9 displays a histogram illustrating the distribution of scores for each method.

Model	Mean Value	Standard Deviation
TDA	0.84	0.01
LKC	0.84	0.01
GeoTop	0.87	0.01

Table 1: Mean and standard deviation of the bootstrap scores for the random forest classifier.

As shown in Table 1, both the TDA and LKC methods exhibit similar classification performances,

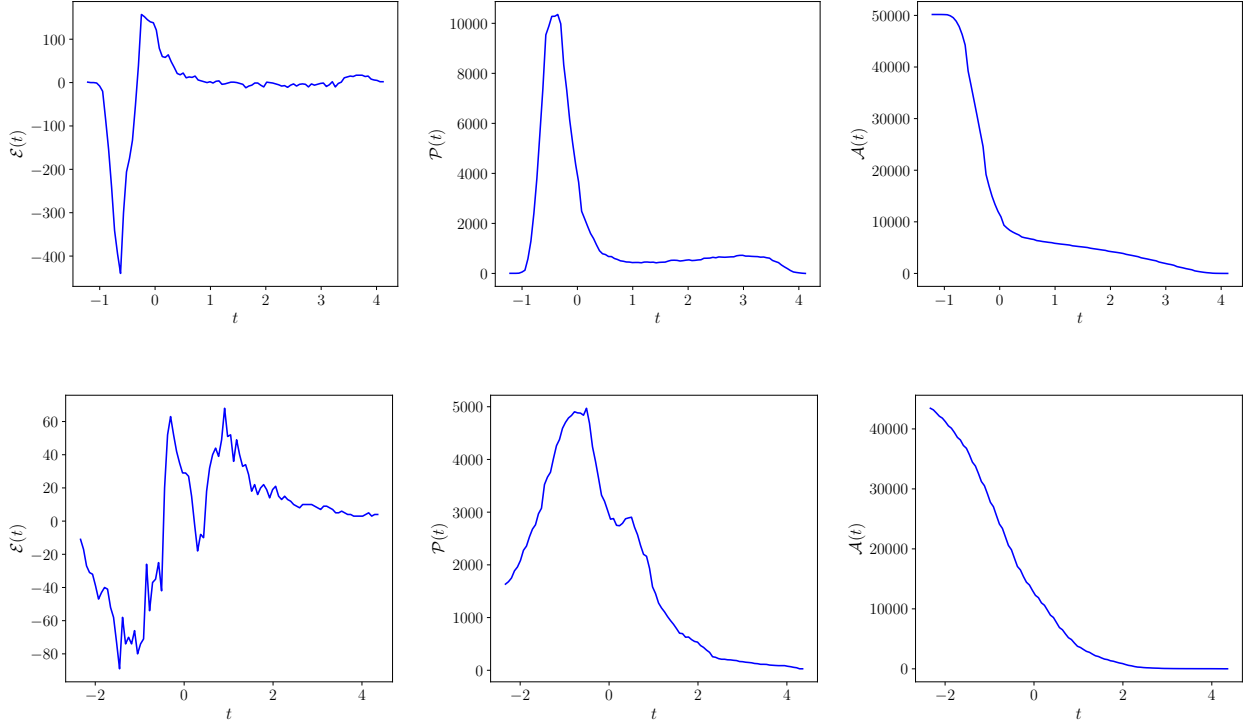


Figure 8: Examples of the LKC functionals computed using 200 thresholds. From left to right: Euler characteristic, perimeter, and area, for grayscale images of benign (first row) and malignant (second row) tumours.

and their combination (GeoTop) results in an average score improvement of two percent. Figure 9, which represents the distribution of scores, reveals that the LKC method performs slightly better, with higher minimum and maximum values. Nonetheless, combining the two methods consistently yields the best results.

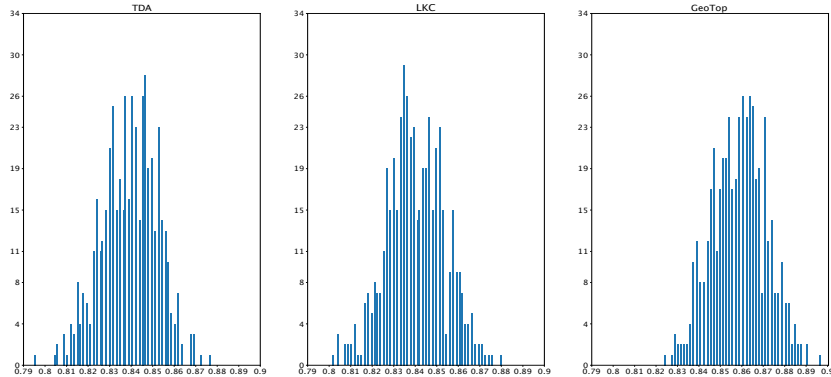


Figure 9: Distribution of the scores obtained from random forest bootstrapping for the three methods.

To further evaluate the prediction results of the three methods, Figure 10 provides an in-depth comparison using average confusion matrices obtained through bootstrapping. The LKC method shows a slightly lower rate of false negatives compared to the TDA method, while the TDA method performs slightly better in terms of false positives. However, the combined GeoTop approach enhances the classification results for both false positives and negatives.

In Table 2, we calculate the mean values of the Adjusted Rand Index (ARI) for the 500 bootstraps

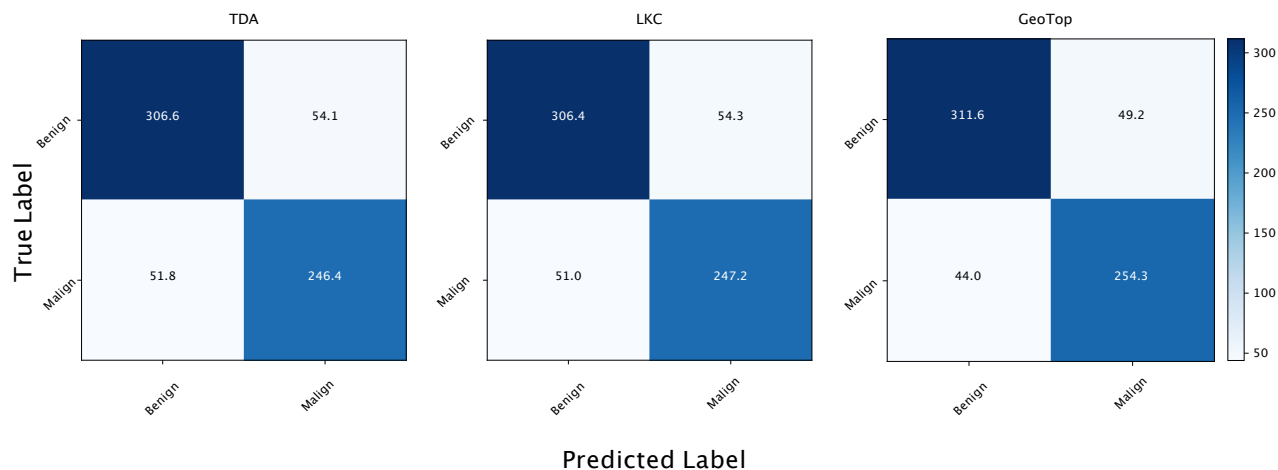


Figure 10: Average confusion matrix for the three methods.

conducted for the three methods (TDA, LKC, and GeoTop). The ARI measures the similarity between two sets of clustered data, ranging from -1 to 1 . An ARI of 1 indicates perfect agreement, 0 represents random agreement, and -1 signifies perfect disagreement. Therefore, higher ARI values indicate closer agreement between the two sets of clusters.

Model	(TDA, LKC)	(LKC, GeoTop)	(TDA, GeoTop)
Mean and std ARI	0.51 (0.04)	0.68 (0.04)	0.67 (0.04)

Table 2: Mean value of the ARI between the predictions of the three methods.

At last, we utilise functions from the `sklearn.metrics` library to compute the average f1-score and precision for the three methods, as shown in Table 3.

Model	TDA	LKC	GeoTop
f1-score	0.82 (0.02)	0.82 (0.02)	0.86 (0.01)
precision	0.82 (0.02)	0.82 (0.02)	0.85 (0.02)

Table 3: Mean f1-score and precision for the three methods.

As shown in Table 3, both the TDA and LKC methods exhibit similar results in terms of f1-score and precision in this classification task. However, combining both methods consistently improves the classification performance.

Illustrative Misclassifications for the Three Methods Below (see Figures 11, 12, and 13), we provide a comparison of the outcomes achieved by the three classification methods to illustrate instances where one method misclassifies images while the others correctly classify them. To simplify, we present only a select few examples.

As observed in the figures presented above, there is no discernable pattern visible to the naked eye that can explain why one method performs better than the others.

4.2 The Synergistic Potential of Topology and Geometry

In our study focused on the application of LKC for classification purposes, we harness the wealth of geometric information extracted from the features under investigation. To enhance our analysis, we propose the

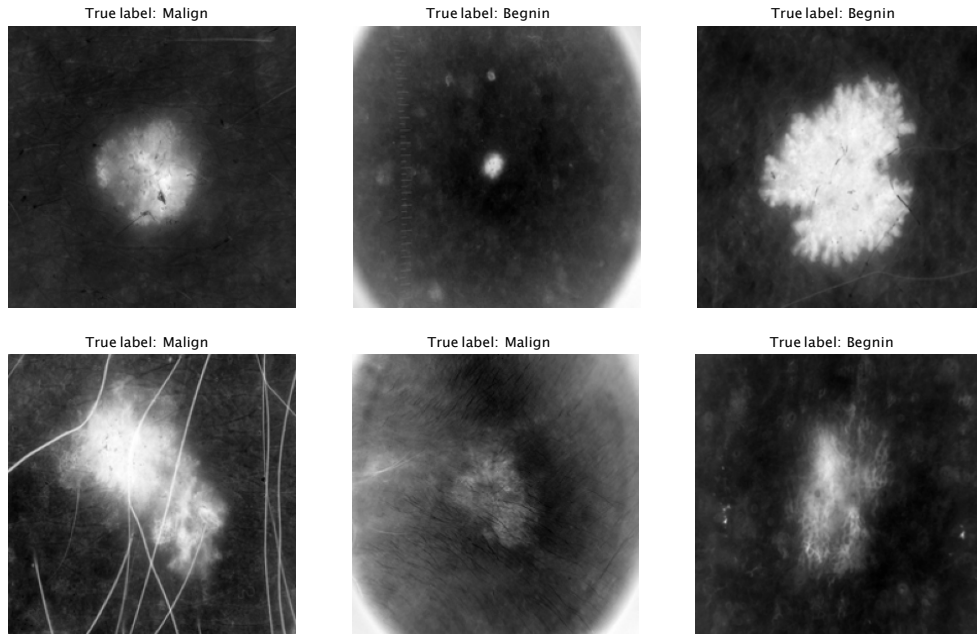


Figure 11: Bottom – Examples of images that are well labeled by TDA but wrongly classified by LKC. Down – Examples of images that are well labeled by LKC but wrongly classified by TDA.

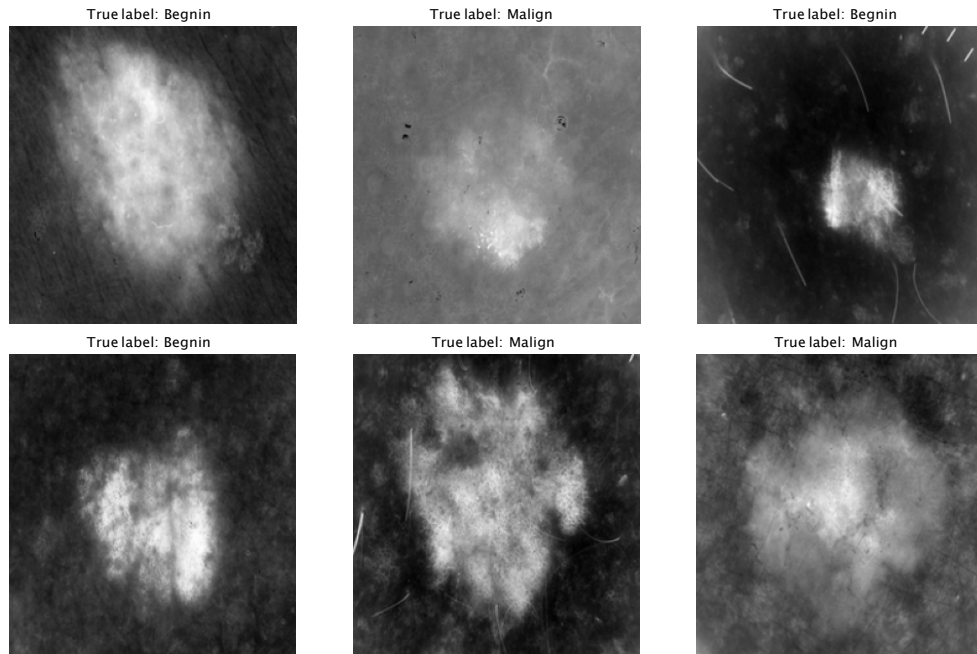


Figure 12: Bottom – Examples of images that are well labeled by GeoTop but wrongly classified by TDA and LKC. Down – Examples of images that are well labeled by LKC and TDA but wrongly classified by GeoTop.

exploitation of the additive nature of LKC and delve into their local aspects. For instance, the perimeter of an excursion set equals the sum of perimeters of connected components within that excursion set, $\mathcal{P}(t) =$

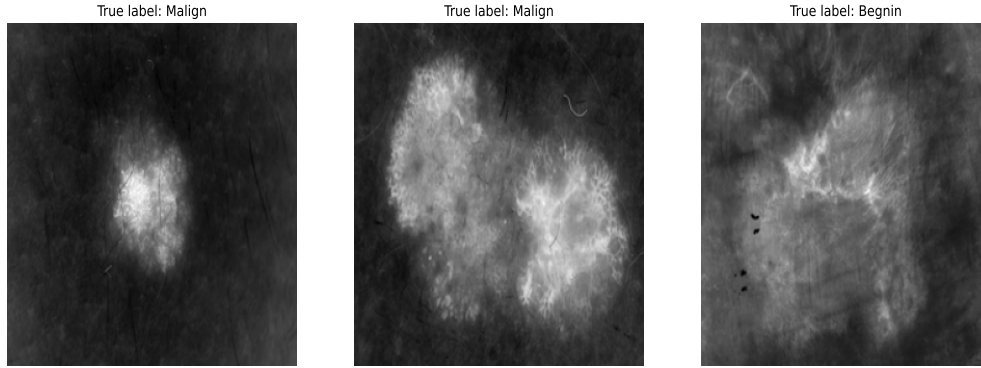


Figure 13: Examples of bad predictions for all three methods.

$\sum_{i \in C_i} \mathcal{P}_i(t)$, where $\mathcal{P}_i(t)$ denotes the perimeter of the i th connected component at threshold level t . By incorporating this local information into TDA, we enrich the dataset with both the geometric attributes of the components and the topological insights offered by their persistence.

Effectively, we amalgamate geometric nuances with pertinent topological characteristics. In practice, we track the existence of each component along with its geometric traits.

Let's examine an image (see the left panel of Figure 14) representing a multivariate Gaussian function with dimensions of 200×200 as an illustrative toy example of the proposed synergy between Topology and Geometry. Within this image, we introduce a square of size 10×10 in the southeast corner, where all the pixels within the square have an intensity equal to the maximum of the Gaussian. When we compute the persistence barcode for the upper-level filtration of this image, we notice that both the Gaussian and the added square result in two connected components of equal significance (as shown in the right panel of Figure 14). Since they share the same intensity, they will both have a similar birth value and approximately the same persistence.

It's important to highlight that while a component may exhibit topological significance, it does not necessarily imply equal importance in terms of its structural and geometrical characteristics. The strength of TDA lies in its ability to capture topological invariants, but it may struggle to differentiate between different structures present in the image when solely relying on the persistence barcode or the persistence diagram.

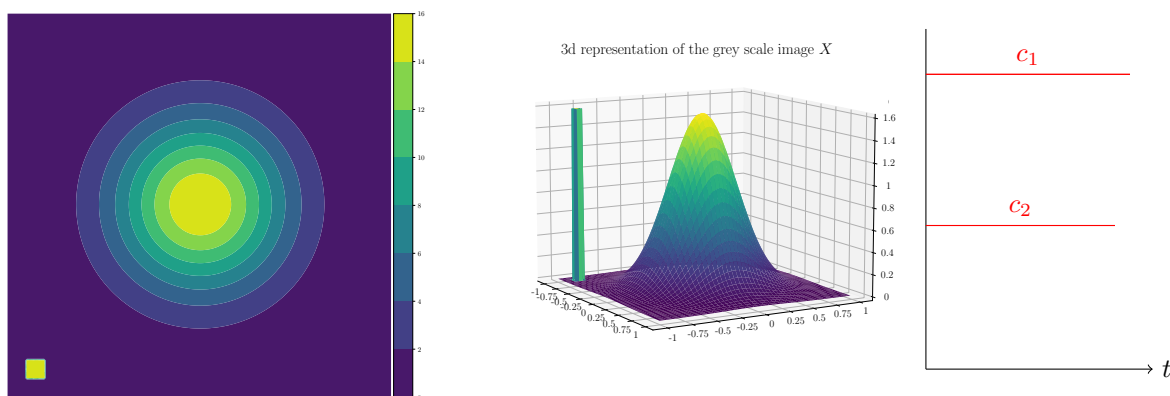


Figure 14: Image of a multivariate Gaussian density and noise and its associated persistence diagram for the upper level filtration.

By tracking the perimeter and area of each connected component of the excursion set while monitoring its persistence, we can gain insights into the significance of the underlying structures within the image and their morphology. This local analysis provides a means to assess the importance of the image's underlying

structures and differentiate them from noise [20].

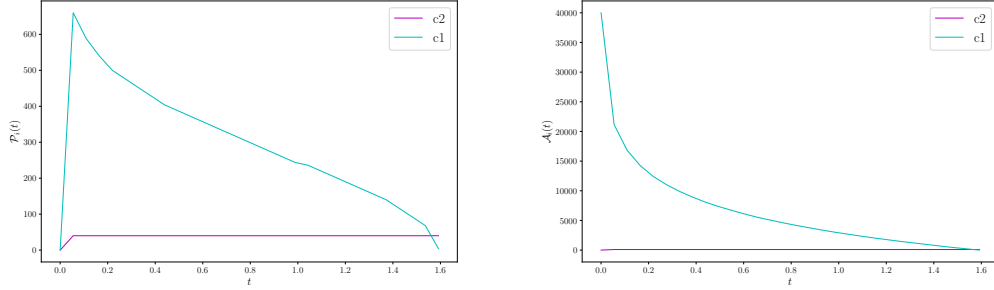


Figure 15: Perimeter (left panel) and area (right panel) of the connected components in orange and blue, along with the total perimeter and area in red.

Figure 15 showcases the geometrical features of the two connected components, namely perimeter and area. As evident, the square exhibits less prominence compared to the Gaussian in the image, making it easily distinguishable as noise. Hence, tracking the Lipschitz-Killing Curvatures (LKC) of connected components enables a detailed analysis of the image’s structure, making it a promising method for exploration.

5 Discussion

In this study, we delved into the realms of TDA and LKC as powerful tools for analysing complex images in the context of biomedical data. Our research aimed to explore their individual and combined potentials for feature extraction and classification in the domain of biomedical image analysis.

Our exploration of TDA unveiled its ability to capture crucial topological features within images. By employing persistent homology and constructing persistence diagrams, we gained insights into the dynamic evolution of topological structures throughout the image filtration process. This dynamic approach allowed us to track the birth and death of topological features, leading to the generation of persistence barcodes and diagrams.

These diagrams provided a unique perspective on image topology, with each point in the diagram representing a topological feature’s birth and death coordinates. Moreover, features with significant persistence emerged as meaningful patterns within the data, while those with low persistence were identified as noise or insignificant fluctuations. This method allowed us to highlight and prioritise relevant structures within the image.

The LKCs, on the other hand, offered a different lens through which to view image data. These curvatures provided concise and insightful summaries of the spatial characteristics of random fields, offering valuable geometric information. In our investigation, we focused on the two-dimensional domain, specifically random fields defined on \mathbb{Z}^2 . The LKCs offered three distinct geometrical features: area, perimeter, and Euler-Poincaré characteristic.

By computing LKCs locally, at different threshold levels, we gained a deeper understanding of the image’s structures. This allowed us to differentiate between various structural elements and noise, ultimately enhancing our classification capabilities.

One of the key findings in our study was the potential for synergy between TDA and LKCs. While each method provided unique insights into the data, combining them proved to be advantageous. By merging topological and geometrical vectors of features, we achieved improved classification results. This combination leveraged both the topological significance of features, as revealed by TDA, and their structural and geometrical characteristics, as quantified by LKCs.

Our classification results demonstrated the effectiveness of TDA, LKCs, and their combination GeoTop. Random forest classifiers were employed to evaluate and compare these methods, with promising outcomes. The TDA and LKC methods exhibited similar classification performances, while the combination of both consistently improved the classification score.

Furthermore, the analysis of confusion matrices revealed that the GeoTop approach reduced the rate of false positives and false negatives, enhancing the overall classification results.

In addition to classification scores, we also assessed the models using ARI, f1-score, and precision. These metrics further supported our findings, highlighting the advantages of combining TDA and LKCs in biomedical image classification tasks.

To gain a deeper understanding of the strengths and limitations of each method, we examined examples of misclassifications. These instances revealed the nuanced nature of biomedical image data and the challenges in distinguishing between structures that may exhibit similar topological properties.

Our study has shed light on the potential of TDA and LKCs in biomedical image analysis. As a future direction, we suggest further exploration of local analysis techniques, where geometrical details are considered in tandem with topological characteristics. This approach could enhance our ability to assess the significance of underlying structures within biomedical images, differentiating between structural elements and noise.

6 Conclusion

In conclusion, our research has demonstrated the value of TDA and LKCs as powerful tools for feature extraction and classification in biomedical image analysis. While TDA captures topological features and patterns, LKCs provide essential geometric information. The combination of both methods has shown promising results in improving classification accuracy, with potential applications in various biomedical multiomics problems. As we continue to unravel the complexities of biomedical data, the fusion of topological and geometrical insights holds great promise for advancing our understanding of the underlying biological processes.

Acknowledgments

We gratefully acknowledge funding from the National Research Association (ANR) (Inflamex renewal 10-LABX-0017 to I Morilla), Consejería de Universidades, Ciencias y Desarrollo, fondos FEDER de la Junta de Andalucía (ProyExec_0499 to I Morilla), ANR MISTIC (ANR-19-CE40-0005) and by the French government, through the 3IA Côte d’Azur Investments in the Future project managed by the National Research Agency (ANR) with the reference number ANR-19-P3IA-0002, and MAP5 laboratory (to M Abaach). The authors wish to acknowledge IHSM for their support.

References

- [1] Robert A. Gatenby, Olya Grove, and Robert J. Gillies. Quantitative imaging in cancer evolution and ecology. *Radiology*, 269(1):8–14, 2013. PMID: 24062559.
- [2] Sara Ranjbar and J. Ross Mitchell. Chapter 8 - an introduction to radiomics: An evolving cornerstone of precision medicine. In Adrien Depeursinge, Omar S. Al-Kadi, and J. Ross Mitchell, editors, *Biomedical Texture Analysis*, The Elsevier and MICCAI Society Book Series, pages 223–245. Academic Press, 2017.
- [3] Yashbir Singh, Colleen M. Farrelly, Quincy A. Hathaway, Tim Leiner, Jaidip Jagtap, Gunnar E. Carlsson, and Bradley J. Erickson. Topological data analysis in medical imaging: current state of the art. *Insights into Imaging*, 14(1):58, Apr 2023.
- [4] A. Garin and G. Tauzin. A topological ”reading” lesson: Classification of mnist using tda. *2019 18th IEEE International Conference On Machine Learning And Applications (ICMLA)*, pages 1551–1556, 2019.
- [5] David Letscher and Jason Fritts. Image segmentation using topological persistence. In Walter G. Kropatsch, Martin Kampel, and Allan Hanbury, editors, *Computer Analysis of Images and Patterns*, pages 587–595, Berlin, Heidelberg, 2007. Springer Berlin Heidelberg.
- [6] Robin Vandaele, Guillaume Adrien Nervo, and Olivier Gevaert. Topological image modification for object detection and topological image processing of skin lesions. *Scientific Reports*, 10(1):21061, Dec 2020.

- [7] Ian Morilla, Philippe Chan, Fanny Caffin, Ljubica Svilar, Sonia Selbonne, Ségolène Ladaigue, Valérie Buard, Georges Tarlet, Béatrice Micheau, Vincent Paget, Agnès François, Maâmar Souidi, Jean-Charles Martin, David Vaudry, Mohamed-Amine Benadjaoud, Fabien Milliat, and Olivier Guipaud. Deep models of integrated multiscale molecular data decipher the endothelial cell response to ionizing radiation. *iScience*, 25(1), 2022.
- [8] Eashwar Somasundaram, Adam Litzler, Raoul Wadhwa, Steph Owen, and Jacob Scott. Persistent homology of tumor CT scans is associated with survival in lung cancer. *Med. Phys.*, 48(11):7043–7051, November 2021.
- [9] Robin Vandaele, Pritam Mukherjee, Heather Marie Selby, Rajesh Pravin Shah, and Olivier Gevaert. Topological data analysis of thoracic radiographic images shows improved radiomics-based lung tumor histology prediction. *medRxiv*, 2022.
- [10] Yu-Min Chung, Chuan-Shen Hu, Austin Lawson, and Clifford Smyth. Topological approaches to skin disease image analysis. In *2018 IEEE International Conference on Big Data (Big Data)*, pages 100–105, 2018.
- [11] Robert J. Adler, Omer Bobrowski, Matthew S. Borman, Eliran Subag, and Shmuel Weinberger. Persistent homology for random fields and complexes. In *Institute of Mathematical Statistics Collections*, pages 124–143. Institute of Mathematical Statistics, 2010.
- [12] Allen Hatcher. *Algebraic topology*. Cambridge Univ. Press, Cambridge, 2000.
- [13] Hengrui Luo and Justin Strait. Combining geometric and topological information for boundary estimation. In *2021 IEEE International Conference on Big Data (Big Data)*, pages 3841–3852, 2021.
- [14] Frédéric Chazal and Bertrand Michel. An introduction to topological data analysis: fundamental and practical aspects for data scientists, 2021.
- [15] Daniel Strömbom. Persistent homology in the cubical setting : theory, implementations and applications, 2007. Validerat; 20101217 (root).
- [16] M. Kratz and S. Vadlamani. Central limit theorem for Lipschitz–Killing curvatures of excursion sets of Gaussian random fields. *Journal of Theoretical Probability*, 2017.
- [17] Dennis Müller. A central limit theorem for lipschitz-killing curvatures of gaussian excursions, 2017.
- [18] H. Biermé and A. Desolneux. The effect of discretization on the mean geometry of a 2d random field. *Annales Henri Lebesgue*, 2021.
- [19] B. Ebner, N. Henze, M. A. Klatt, and K. Mecke. Goodness-of-fit tests for complete spatial randomness based on Minkowski functionals of binary images. *Electronic Journal of Statistics*, 12(2):2873–2904, 2018.
- [20] Mariem Abaach, Hermine Biermé, and Elena Di Bernardino. Testing marginal symmetry of digital noise images through the perimeter of excursion sets. *Electronic Journal of Statistics*, 15(2):6429–6460, 2021.